HHS Public Access

Author manuscript

Colloids Surf A Physicochem Eng Asp. Author manuscript; available in PMC 2018 September 20.

Published in final edited form as:

Colloids Surf A Physicochem Eng Asp. 2017 September 20; 529: 119–127. doi:10.1016/j.colsurfa.2017.05.058.

Processing-Size Correlations in the Preparation of Magnetic Alginate Microspheres Through Emulsification and Ionic Crosslinking

Andrew R. Garcia[1], **Christopher Lacko**[2], **Catherine Snyder**[3], **Ana C. Bohórquez**[2], **Christine E. Schmidt**[2], and **Carlos Rinaldi**[1,2]

[1]Department of Chemical Engineering, University of Florida, 1030 Center Drive, Gainesville, FL 32611

[2]J. Crayton Pruitt Family Department of Biomedical Engineering, University of Florida, 1275 Center Drive, Biomedical Sciences Building JG-56, P.O. Box 116131, Gainesville, FL 32611-6131

[3]Department of Materials Science and Engineering, University of Florida, 100 Rhines Hall P.O. Box 116400, Gainesville, FL 32611-6400

Abstract

Magnetic alginate microspheres are biocompatible due to their alginate matrix, and motion-controllable by applied magnetic fields due to their magnetic character. Therefore, they have the potential of being used as vessels to a broad variety of materials, including drugs and therapeutic agents, facilitating entry to biological systems in a relatively non-invasive manner. Here, magnetic alginate microspheres were prepared through an emulsification and ionic cross-linking process, where a mixture of alginate and iron oxide magnetic nanoparticles was initially dispersed in a continuous phase, followed by gelation of this dispersed phase into microspheres by cross-linking the dispersion with calcium ions. The resulting magnetic alginate microspheres were found to be superparamagnetic and to respond to applied magnetic fields by chain formation. The effect of shear rate, alginate concentration, and magnetic nanoparticle concentration on microsphere size was investigated with the aim to control the size of microspheres with respect to process and formulation parameters. Two of these parameters, shear rate and alginate concentration, were used to correlate experimental results with a theoretical model for the case where the dispersed phase is more viscous than the continuous phase.

Graphical abstract

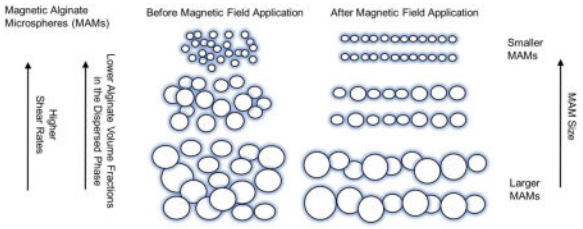

Keywords

magnetic microparticles; magnetic nanoparticles; alginate; emulsification

Introduction

Alginate is an anionic copolymer derived from brown algae and composed of a combination of 1–4 linked β-D-mannuronate (M) and α-L-guluronate (G). This copolymer has a wide range of applicability in the food and biotechnology industries due to its biocompability and unique capacity to be used as a matrix that can incorporate a variety of molecules and particles by gelation [1]. Alginate gelation occurs through a phenomenon known as cooperative binding, where the alginate chains attain a more rigid packing under the presence of a divalent cation that binds with the polar groups of alginate to form an ionic crosslink [2]. Generally, calcium ions are used to induce cooperative binding and thus make alginate spheres ranging from nanometers to centimeters containing materials such as antigens [3, 4], proteins [5, 6], stem cells [7], and magnetic nanoparticles [8–14].

Magnetic alginate microspheres, alginate microspheres containing magnetic materials, have targeted delivery applications because they can be manipulated by externally applied magnetic fields. When drugs or therapeutic agents are introduced to alginate microspheres, precise targeting can be achieved by physical manipulation of the magnetic alginate drug carrier [8]. Magnetic alginate microspheres have been made by emulsification [8, 15], injection in calcium solution [10], and through the use of microfluidic devices [9]. Magnetic alginate beads have also been prepared by in situ precipitation of iron oxide nanoparticles inside alginate beads [16].

Here we present a study of the correlation between preparation conditions and magnetic alginate microsphere size obtained through emulsification and ionic crosslinking. The effects of magnetic nanoparticle concentration in the alginate phase and shear rate during emulsification on microsphere size were studied. These variables were correlated using theoretical models for the emulsification process, obtaining good agreement between experiments and expectations from the models.

Materials And Methods

2.1. Materials

Alginic acid from the brown algae *Laminaria digitata* (viscosity of 350–500 cP at 1 % w/w and a mannuronic to guluronic acid (M:G) ratio of 1.5–1.6 according to the supplier),

calcium chloride dihydrate (f.w. 147.01 g/mol), Span 80, Tween 80, mineral oil, and 1-octadecene were obtained from Fisher Scientific.

2.2. Synthesis of Iron Oxide Magnetic Nanoparticles

Iron oxide nanoparticles (Fe_3O_4) were synthesized by the co-precipitation method [17] following the procedure described by Herrera et al. [18], with minor variations. Briefly, coprecipitation of Fe^{+3} (iron (III) chloride hexahydrate), and Fe^{+2} (iron (II) chloride tetrahydrate) salts in an alkaline medium took place with a Fe^{+3}/Fe^{+2} ratio equal to 2.73 under a N_2 atmosphere at 80 °C for 1 hour. After that, particles were centrifuged for 10 min at 1500 rpm and decanted from the supernatant using a magnet. Iron oxide particles were then peptized with tetramethylammonium hydroxide ($(CH_3)_4NOH$) as a peptization agent via centrifugation for 10 min at 1500 rpm. The resulting black sticky paste was placed in the vacuum oven at 60 °C overnight. Particles were then stored in the refrigerator at 4°C until use.

2.3. Preparation of Magnetic Alginate Microspheres by Emulsification

Magnetic alginate microspheres were made by an emulsification and ionic cross-linking process illustrated in Figure 1, adapted from the work of Jay et al. [19] and Jay and Saltzman [20]. With the aim of controlling microsphere size through manipulation of process and formulation parameters, four different sets of experiments were conducted, where a single factor was varied while keeping the others constant (Table S1 in Supporting Information).

Two different mixers were used to make alginate microspheres. A Fisher Scientific PowerGen 125 homogenizer with a rotor rotation-frequency range of 8,000–30,000 rpm and a Silverson L5M-A laboratory mixer with a rotor rotation-frequency range of 0–10,000 rpm. The geometry of rotor-stator mixers can be simplified as two concentric cylinders to calculate the theoretical shear rate as a function of rotor and stator diameter, as well as frequency.

$$\dot{\gamma}=\frac{N}{30}\frac{\pi D}{D_i - D} \quad (1)$$

where D and D_i are the rotor and stator diameters, respectively, and N is the mixing frequency in rpm [21]. To consolidate the results obtained from the different mixers, the rotor rates generated by both mixers were transformed to shear rates using equation (1).

In a typical synthesis, 1 mL of a viscous alginate solution with an initial concentration that varied from 20–80 mg/mL was mixed with 1 mL of a ferrofluid with a magnetic nanoparticle (MNP) concentration that varied in the range of 16–300 mg MNPs per mL water. Additionally, 8 mL of a mineral oil solution containing 5% (v/v) of span 80 was prepared and mixed using a rotor-stator homogenizer applying a shear rate that varied from 700–14,000 s^{-1}. The shear rate was kept constant throughout homogenization. With the mineral oil solution under homogenization, the alginate-ferrofluid solution was added and emulsified until it appeared homogeneous. After this step, 0.5 mL of an aqueous solution with 30% (v/v) tween 80 was added to the emulsion and mixed with the homogenizer. After

achieving a uniform mixture, the dispersed phase was ionically cross-linked to form microspheres by adding 2 mL of a 700 mM $CaCl_2$ solution at a rate of 3 mL per minute while homogenizing. Mixing was then stopped and the emulsion combined with 10 mL of 100% ethanol, vortexed, and centrifuged at 4,000 rpm at 20 °C using an Eppendorf 5430R centrifuge with an F-35-6-30 rotor for one minute. After centrifugation, the supernatant was separated from the precipitate by magnetic decantation. Afterwards the precipitate was washed in 25 mL of ethanol, followed by centrifugation at 4,000 rpm for one minute. These magnetic decantation and ethanol washing steps were repeated until excess amounts of oil and surfactant were removed from the precipitate. The resulting precipitate, containing the microspheres, was then air dried for a period of 6 to 8 hours, followed by lyophilization using a Labconco® FreeZone 4.5 Liter Cascade Benchtop Freeze Dry System at pressures below 0.12 mPa and temperatures of −53°C or below.

2.4. Microsphere Characterization

Scanning electron micrographs of the microsphere samples were obtained using a Phenom Pro Desktop Scanning Electron Microscope (SEM) and a FEI Phillips XL40 Field Emission Gun Scanning Electron Microscope (FEG-SEM). For these analyses we prepared samples of microspheres by placing a small amount of lyophilized microspheres on the SEM tape of an SEM stub, making sure that the microspheres have adhered properly to the tape. This was followed by sputter coating the sample with gold as a conductive material.

ImageJ (distributed by the NIH) [22] and Adobe Photoshop version CS6 were both used to quantify microsphere size by sampling individual microspheres from SEM micrographs. To obtain an accurate size distribution, at least 80 microspheres were sampled per experiment.

A superconducting quantum interference device (SQUID) magnetometer (Quantum Design SQUID-MPMS3) was used to characterize the magnetization of microsphere samples under applied magnetic fields. Microsphere samples were analyzed by mounting lyophilized microspheres in gelatin capsules. Magnetization measurements were normalized by lyophilized sample mass. The diamagnetic background due to the organic (alginate) components in the sample was subtracted. The saturation magnetization for the samples was estimated from the high-field asymptote of the background-subtracted magnetization measurements.

Iron content in the particle stock and magnetic alginate microspheres was estimated spectrophotometrically using the *o*-phenanthroline assay. Iron oxide content of the microsphere samples was measured using a colorimetric absorbance assay. The microspheres were first dispersed in 100 mM ethylenediaminetetraacetic acid for 24 hours at a concentration of 10 mg/ml to homogenize the samples before measurement. Afterwards, 10 ul aliquots were taken in triplicate from each sample and digested in 1 ml of 70% Nitric Acid (Fisher) at 101 °C for twelve hours to degrade alginate in the assay. Solutions of 8.06 M hydroxylamine hydrochloride, 1.22 M sodium acetate, and 13 M 1,10-phenanthroline monohydrate were prepared. Iron standards of known concentrations were prepared by diluting an iron standard for ICP (Sigma) to create a calibration curve. After digestion, 10 μl aliquots were taken from each nitric acid sample, placed into 1.5 mL glass vials and heated to 115 °C to evaporate all samples. To each glass vial, 46 μl of deionized distilled (dDI)

water was added. The iron standards were diluted by adding 36 μl of dDI water. Aliquots of 30 μl of hydroxylamine were added to each sample to reduce iron samples from Fe^{+3} to Fe^{+2}. After an hour, 49 μl of sodium acetate and 75 μl of 1,10-phenanthroline are added to each sample. Formation of iron (II)-orthophenanthroline caused the samples to turn an orange-red color. After loading 100 μl of sample into wells on a 96-well quartz plate, the absorbance values were read at 508 nm using a SpectraMax® M5 Multimode plate reader. Using the iron standards, the concentration of the iron was related to the absorbance value, allowing the iron concentration of the unknown samples to be quantified. Iron oxide concentrations were estimated from the iron measurements by making a correction based the chemical formula of magnetite (Fe_3O_4). These measured concentrations were then compared to the initial weight-based concentration of the samples of 10 mg/ml to determine a mass fraction of iron oxide in the magnetic alginate microsphere samples.

2.5. Theoretical Background Used for Microsphere Size Analysis

To correlate microsphere size with respect to process and formulation parameters, we have fitted some of our experimental data to a theoretical model that predicts emulsion droplet size under our emulsion conditions. The equation by Leng and Calabrese was used because it describes the size of dispersed droplets in turbulent flow for emulsion systems with a viscous dispersed phase [23]

$$d = C_1(\rho_c\rho_d)^{-3/8}\mu_d{}^{3/4}\varepsilon^{-1/4} \quad (4)$$

Since emulsifications with high viscosity dispersed phases typically have energy dissipation rates (W/kg) independent of flow rate, we assume the energy dissipation rate is equal to the stirred tank power term, $P = \mathrm{Po}\rho_c N^3 D^5$, which corresponds to the power required to rotate the rotor to overcome fluid resistance [24]. Defining the energy dissipation rate in this manner and using equation (1) we obtain the following expression

$$\varepsilon = \mathrm{Po}\rho_c \overline{D} Q^{-1}\dot{\gamma}^3 \quad (5)$$

Where $\bar{D} = (D_i - D)^3 D^2$ is a function of the stator and rotor diameters of the homogenizer and Q is a constant with units of mass. Using equation (5) in combination with the droplet size equation (4) and combining all terms that are kept constant during the experiments, the following expression is obtained

$$d = C_2\left(\frac{\mu_d}{\dot{\gamma}}\right)^{3/4} \quad (6)$$

$$C_2 = C_1(\rho_c\rho_d)^{-3/8}(\mathrm{Po}\rho_c\overline{D}Q^{-1})^{-1/4} \quad (7)$$

Equation (6) can be used to estimate microsphere size because ionic crosslinking of the dispersed phase occurs during the emulsification process. For cases where the dispersed phase viscosity μ_d could not be obtained, an equation can be derived as an approximation that relates to the alginate volume fraction ϕ instead. By definition, the intrinsic viscosity $[\mu]$ attains a constant value at the limit where volume fraction approaches 0

$$[\mu]=\lim_{\phi\to 0}\frac{\mu-\widehat{\mu_0}}{\widehat{\mu_0}\,\phi} \quad (8)$$

Low alginate volume fractions were used for all microspheres [ϕ < 2%], therefore, we can assume the dynamic viscosity μ_d is given by

$$\mu_d=\widehat{\mu_0}\,(1+[\mu]\phi) \quad (9)$$

A typical value for [μ] of an alginate-water system determined through the Huggins method is 1,269 [25]. For the special case where $[\mu]\phi > 1$, equation (6) can be written as

$$d=C_3\left(\frac{\phi}{\dot{\gamma}}\right)^{3/4} \quad (10)$$

$$C_3=C_2(\widehat{\mu_0}\,[\mu])^{3/4} \quad (11)$$

In the present case, the values for the constant coefficient C_3 and for the exponents of ϕ and $\dot{\gamma}$ will be determined by a power law fit of the following form and compared with equation (10):

$$d=e^a\phi^x\dot{\gamma}^y \quad (12)$$

Equation (12) can be used to relate both emulsion droplet and microsphere size to emulsification process and material conditions for the case of a viscous dispersed phase.

3. Results And Discussion

3.1. Effect of Shear Rate and Alginate Loading on Microsphere Size Using a High Viscosity Continuous Phase

A series of magnetic alginate microsphere preparations were investigated to assess the effect of different process parameters on microsphere size. A representative SEM image is shown in Figure 2. Here we show the results for microsphere preparations from two different sets, sets 1 and 2 from Table S1 (Supporting Information), to make inferences on how

microsphere size distributions are affected by shear rate ($\dot{\gamma}$) and by alginate volume fraction in the dispersed phase ϕ.

The size distributions of microspheres from set 1 are shown in Figure 3. For this set we prepared a series of microspheres under different shear rates while keeping the alginate volume fraction in the dispersed phase constant at 0.984% v/v, using a magnetic nanoparticle concentration of 16 mg/mL, and mineral oil as the continuous phase. The microsphere size distributions were clearly affected by shear rate. At high shear rates, the microsphere distributions are relatively narrow, and the average microsphere diameter is smaller. In contrast, lower shear rates resulted in larger microspheres with increased polydispersity. Such stratification in microsphere sizes under low shear rate can be attributed to low power mixing at significantly low shear rates. Under this condition, the flow profile generated by the homogenizer is restricted to a small region close to the homogenizer that does not encompass the whole volume that needs to be homogenized, resulting in non-uniform mixing and a non-uniform microsphere size distribution.

A second set of experiments, set 2 from Table S1 (Supporting Information), was designed to investigate the effect of alginate concentration on microsphere size distributions. Microsphere preparations were made by changing the alginate volume fraction in the dispersed phase while keeping the shear rates constant at 9400 s^{-1}, using a magnetic nanoparticle concentration of 16 mg/mL, and mineral oil as the high viscosity continuous phase.

The size distribution data in Figure 4 demonstrate increasing microsphere diameters with increasing alginate volume fraction In this set of experiments, the size distributions are uniformly broad, indicating greater polydispersity than those from the highest shear rate microsphere preparations shown in Figure 3. However, there is no apparent dependency between polydispersity and the alginate volume fraction, unlike the correlation between polydispersity and shear rate demonstrated in the previous experiment (Figure 3). This suggests that, under the tested range of ϕ, microsphere size can be tuned by ϕ without major changes in the spread of the size distribution.

The power law from equation (12) was used to relate microsphere size to shear rate and alginate volume fraction in the dispersed phase. To estimate the microsphere size with respect to these two factors, the exponents from equation (12) were determined from a single least squares bivariate fitting of the model with the median diameter data from sets 1 and 2 from Table S1 (Supporting Information). From this global bivariate fit we obtained a regression coefficient (R^2) for the regression between experimental and correlated median diameters of 0.976, and a 95% confidence interval of 0.428 μm, which was calculated from the critical t value at a 95% significance level and the standard error of the experimental data. Figures 5 and 6 compare this theoretical fit to experimental data from sets 1 and 2 respectively, each of which may be perceived as a 2-dimensional slice from the bivariate fit where one factor was varied at a time. In the plots from Figures 5 and 6, the dots represent median values and solid vertical dashed lines represent the interquartile range (IQR); these vertical lines extend from the first quartile (Q1) to the third quartile (Q3) from bottom to top. Dashed lines span the values from the ends of the IQR to the ends of the inner fences

(Q1−1.5*IQR and Q3+1.5*IQR for the lower and upper fences, respectively). And lastly, the crosses represent outliers falling beyond the fences. Medians and interquartile ranges (IQR) were used as size distribution descriptors, because most microsphere size distributions were not found to be uniform.

The exponent value of $\dot{\gamma}$ determined by the fit was −0.64 with a standard error estimate of 0.03, which is close albeit smaller than the theoretical exponent value of −0.75 from equation (12). Using data from microsphere preparations emulsified under conditions that were not in fully turbulent flow may have caused this discrepancy. For the first set of microsphere preparations where shear rate was varied (set 1 from Table S1 in Supporting Information), dispersions were produced with estimated rotor Reynolds numbers $Re = \rho_c N D^2/\mu_c$ in the range of 260-5,300. Prior investigations of 18 different flow regimes for a circular Couette system suggested that transitions between different flow regimes are dependent on both the inner- and outer-cylinder Reynolds numbers, Re_i and Re_o, respectively [26]. Because the outer cylinder of the homogenizers used for these microsphere preparations are stators, we define $Re_o = 0$ and $Re_i = Re$. For such a case, the flow regime is azimuthal laminar (AZI) for $0 < Re < 120$, and passes through an initial instability, the Taylor vortex flow (TVF), and two different oscillating vortex flows (WVF and MVV) before reaching turbulent Taylor vortex flow (TTV) at a $Re > 1{,}370$ [26]. Consequently, microsphere preparations made with the three lowest shear rates shown in Figure 5, had $Re < 1{,}370$ and deviated the most from the assumption of turbulent flow.

The exponent value of ϕ determined by the fit was 0.75 with a standard error estimate of 0.17. Despite this determined coefficient being in agreement with its theoretical value of 0.75 from equation (12), its standard error is relatively high.

While the results demonstrate that microsphere size can be tuned by varying alginate concentrations, there is a relatively narrow range within which the concentration of alginate can be varied. The high viscosity alginate used makes it increasingly challenging to disperse alginate in aqueous solutions at concentrations above those used for these experiments. The choice of a less viscous alginate material is also expected to alter the microsphere size, as it is directly related to dispersed phase viscosity by equation (6).

3.2. Effect of Shear Rate on Microsphere Size Using a Low Viscosity Continuous Phase

Seeing how the density of the continuous phase ρ_c is inversely proportional to microsphere size by equation (4), we hypothesized that replacing the mineral oil continuous phase with 1-octadecene, a lower density and lower viscosity oil, would result in the production of larger microspheres. Therefore, a series of experiments using 1-octadecene as the continuous phase with varying shear rates was conducted. For these experiments, the alginate volume fraction and magnetic nanoparticle concentration were fixed to 0.984% v/v and 16 mg/mL, respectively.

The resulting microsphere size distributions from these experiments are shown in Figure 7. From these distributions one can observe high polydispersity and no apparent effect of varying shear rates on microsphere size under these conditions. Under the current operating

conditions, we hypothesize that shear rate does not alter microsphere size because of the inability of the homogenizers to uniformly disperse the emulsions.

For the case of simple shear flow, the ratio of viscous to inertial forces necessary for a droplet to break is related to the viscosity ratio between dispersed and continuous phases $p=\frac{\mu_d}{\mu_c}$ [27, 28]. It has been reported that breakage cannot be caused by simple shear flow at viscosity ratios $p > 4$ [28, 29]. The viscosity of mineral oil is 56 cP, compared to 1-octadecene, which is 4.315 cP. For the alginate used, according to the supplier, at a mass fraction of 1% (w/w) [or ϕ = 0.63% (v/v)], the viscosity is 350 – 550 cP. This results in $6.3 < p < 9.8$ for mineral oil as the continuous phase and $81 < p < 130$ with 1-octadecene, with higher p values for alginate mass fractions going above 1%. This shows that neither of the continuous phases studied herein would be able to yield viscosity ratios sufficiently low to cause droplet breaks for the case of simple shear flow.

For the case of turbulent flow, the stress acting to deform a droplet is given by Kolmogorov's theory of local turbulence isotropy [23], where droplet breakup is caused by the energy of turbulent eddies of length scales given by the Kolmogorov microscale:

$$\eta=(\nu_c^3/\varepsilon)^{1/4} \quad (11)$$

Using this expression and equation (5), a decrease in the scale of the eddies implies a stronger local shear to break droplets into smaller units. Similarly, the scale of turbulent eddies can be decreased by increasing the shear rate, though the effectiveness of the eddies in breaking droplets reaches a limit when the shear rate causes the eddies to become so small that their energy is lost as heat by viscous dissipation [30].

This set of microspheres was dispersed under the mechanism of turbulent flow, as the Reynolds number $\mathrm{Re} = \rho_c N D^2/\mu_c$ ranged from 21,000–86,000. Despite theoretically allowing for larger microsphere generation compared to mineral oil, we were not able to modulate microsphere size with shear rate using 1-octadecene as the continuous phase. We hypothesize the viscosity of 1-octadecene is too low, causing sufficiently small turbulent eddies for viscous dissipation, energy loss, and resulting in non-uniform dispersion.

3.3. Magnetic Properties of Magnetic Alginate Microspheres

Equilibrium magnetization measurements at 300K, normalized by the total mass of dry microspheres, were obtained for two magnetic alginate microsphere samples and a dry magnetic nanoparticle (MNP) stock sample used to make the microspheres. These are shown in Figure 8. These curves show that the microsphere samples exhibit superparamagnetic behavior because their magnetization curves have zero coercivity and remanence.

The saturation magnetization of the magnetic alginate microspheres was a function of the concentration of iron oxide nanoparticles used in the alginate solution during emulsification. We estimated the iron oxide content in the microspheres in three ways. First, we directly measured the iron content using the *o*-phenanthroline assay and converted the iron content

into an iron oxide mass fraction using the stoichiometry of magnetite and known total mass of microspheres in the sample. Second, we calculated the iron oxide mass fraction by the ratio of the saturation magnetization (in units of Am^2/kg) determined from the SQUID measurements to that of bulk magnetite (86 Am^2/kg [31]). Finally, we estimated the expected iron oxide mass fraction based on the ratio of iron oxide to alginate masses used in the alginate dispersed phase during emulsification. Table 1 shows all three values for the iron oxide mass fraction in two representative magnetic alginate microsphere samples, prepared with different concentrations of iron oxide nanoparticles. The excellent agreement between the three values suggest good incorporation of the iron oxide nanoparticles into the magnetic alginate microspheres.

A microsphere sample with high magnetic nanoparticle concentration was also observed through optical microscopy. Figure 9 shows how, in aqueous suspension, magnetic alginate microspheres are capable of forming columnar chains under an external magnetic field. In the absence of the magnetic field, the microspheres form a spatially random distribution.

Microspheres made with different magnetic nanoparticle concentrations were also characterized by SEM. Within the explored ranges, microsphere size distributions appear to be independent of the concentration of magnetic nanoparticles added to the dispersed phase (Figure 10). Even though the mass of magnetic nanoparticles added to the dispersed phase were varied in a broader range [16–300 mg] than those of alginate [20–80 mg], the experiments show that microsphere size correlates strongly with alginate and not with magnetic nanoparticle concentration. This may be attributed to the small intrinsic viscosity of ferrofluids compared to alginate, making the contributions of magnetic nanoparticles negligible to the dispersed phase viscosity, and therefore, microsphere size.

4. Conclusions

Alginate microspheres with incorporated magnetite were made through an emulsification process where a viscous aqueous phase containing alginate and a ferrofluid were dispersed in a continuous phase, followed by ionic crosslinking of the dispersed phase into microspheres and removal of the continuous phase. Magnetic measurements for a representative set of magnetic alginate microspheres showed they exhibited superparamagnetic behavior. Magnetic microspheres were also observed to form columns in fluid under the application of a magnetic field.

The mechanism of emulsification in the preparation of these magnetic alginate microspheres has been investigated, and the microsphere size was correlated using a theoretical model used for determining emulsion droplet size in a turbulent flow emulsification process [23]. Microsphere size was found to be tunable with both shear rate and alginate volume fraction when mineral oil was used as a high viscosity continuous phase. The determined power law exponent of shear rate had a low standard error value, but did not compare closely to its theoretical value, perhaps due to unfavorable laminar flow at the lowest shear rates employed to make microspheres. In contrast, the determined power law exponent of alginate volume fraction was in close agreement with its theoretical value.

When 1-octadecene was used as a low viscosity continuous phase, increased polydispersity was observed in every preparation, and no trend was found between microsphere size and shear rate. This is thought to be a result of unfavorable flow conditions for proper emulsion dispersion caused by the kinematic viscosity parameters and significantly high shear rates, which made the scale of eddies, as determined by the Kolmogorov length scale η, sufficiently small for them to lose their energy as heat.

The study presented in this paper shows the extent of particle size controllability of magnetic alginate microspheres made through an emulsification process under the currently employed conditions. As the mechanism of emulsion droplet formation using rotor-stator mixers is well established, this paper provides a methodology that may be used to develop magnetic alginate microsphere preparations with different size parameters and thus, with the potential to incorporate materials of different sizes.

Supplementary Material

Refer to Web version on PubMed Central for supplementary material.

Acknowledgments

The authors thank Prof. Josephine Allen for advice on SEM characterization, and Ishita Singh and Shehaab Savliwala for help characterizing magnetic properties of the samples. Research reported in this publication was supported by the National Institute of Neurological Disorders and Stroke of the National Institutes of Health under Award Number 1R21NS093239-01. The content is solely the responsibility of the authors and does not necessarily represent the official views of the National Institutes of Health.

Nomenclature

$\mathbf{D}$	rotor diameter
$\mathbf{D_i}$	stator diameter
$\mathbf{D_{pgv}}$	magnetic core volume median diameter
$\mathbf{đ}$	magnetic particle diameter
$\mathbf{d}$	droplet / microsphere diameter
$\mathbf{H}$	Magnetic Field
$\mathbf{k}$	Boltzmann constant
$\mathbf{M}$	Magnetization
$\mathbf{M_d}$	Bulk Magnetization
$\mathbf{M_s}$	saturation magnetization
$\mathbf{m}$	magnetic moment magnitude of a magnetic particle
$\mathbf{N}$	mixing frequency
$\mathbf{P}$	Power

Q	a constant with units of mass
T	Temperature
Z	magnetic nanoparticle mass per volume of dispersed phase
$\dot{\gamma}$	shear rate
ε	energy dissipation rate
[μ]	intrinsic viscosity
μ	dynamic viscosity
μ_0	permittivity
$\widehat{\mu_0}$	viscosity of solvent
μ_d	viscosity of the dispersed phase
ν_c	kinematic viscosity of the continuous phase
ρ_c	density of the continuous phase
ρ_d	density of the dispersed phase
σ_g	geometric deviation
ϕ	alginate volume fraction in the dispersed phase
$\hat{\phi}$	magnetic volume fraction
$Po = P/\rho_c N^3 D^5$	Power number
$Re = \rho_c N D^2/\mu_c$	Reynolds number

References

1. Rousseau I, Le Cerf D, Picton L, Argillier JF, Muller G. Entrapment and release of sodium polystyrene sulfonate (SPS) from calcium alginate gel beads. European Polymer Journal. Dec.2004 40:2709–2715.
2. Grant GT, Morris ER, Rees DA, Smith PJC, Thom D. Biological interactions between polysaccharides and divalent cations: the egg-box model. FEBS Letters. 1973; 32:195–198.
3. Cho NH, Seong SY, Chun KH, Kim YH, Kwon IC, Ahn BY, et al. Novel mucosal immunization with polysaccharide-protein conjugates entrapped in alginate microspheres. J Control Release. Apr 30.1998 53:215–24. [PubMed: 9741929]
4. Lemoine D, Wauters F, Bouchend'homme S, Preat V. Preparation and characterization of alginate microspheres containing a model antigen. International Journal of Pharmaceutics. Dec 30.1998 176:9–19.
5. Zhai P, Chen XB, Schreyer DJ. Preparation and characterization of alginate microspheres for sustained protein delivery within tissue scaffolds. Biofabrication. Mar.2013 5
6. Nesamony J, Singh PR, Nada SE, Shah ZA, Kolling WM. Calcium alginate nanoparticles synthesized through a novel interfacial cross-linking method as a potential protein drug delivery system. Journal of Pharmaceutical Sciences. Jun.2012 101:2177–2184. [PubMed: 22411606]

7. Yao R, Zhang R, Luan J, Lin F. Alginate and alginate/gelatin microspheres for human adipose-derived stem cell encapsulation and differentiation. Biofabrication. Jun.2012 4:025007. [PubMed: 22556122]
8. Ciofani G, Raffa V, Menciassi A, Cuschieri A, Micera S. Magnetic alginate microspheres: system for the position controlled delivery of nerve growth factor. Biomed Microdevices. Apr.2009 11:517–27. [PubMed: 19067172]
9. Yeh CH, Zhao QL, Lee SJ, Lin YC. Using a T-junction microfluidic chip for monodisperse calcium alginate microparticles and encapsulation of nanoparticles. Sensors and Actuators a-Physical. Apr 29.2009 151:231–236.
10. Xu P, Guo F, Huang J, Zhou S, Wang D, Yu J, et al. Alginate-based ferrofluid and magnetic microsphere thereof. Int J Biol Macromol. Dec 01.2010 47:654–60. [PubMed: 20797404]
11. Degen P, Zwar E, Schulz I, Rehage H. Magneto-responsive alginate capsules. J Phys Condens Matter. May 20.2015 27:194105. [PubMed: 25923881]
12. Joshi A, Solanki S, Chaudhari R, Bahadur D, Aslam M, Srivastava R. Multifunctional alginate microspheres for biosensing, drug delivery and magnetic resonance imaging. Acta Biomater. Nov. 2011 7:3955–63. [PubMed: 21784175]
13. Degen P, Leick S, Siedenbiedel F, Rehage H. Magnetic switchable alginate beads. Colloid and Polymer Science. Jan.2012 290:97–106.
14. Finotelli PV, Da Silva D, Sola-Penna M, Rossi AM, Farina M, Andrade LR, et al. Microcapsules of alginate/chitosan containing magnetic nanoparticles for controlled release of insulin. Colloids Surf B Biointerfaces. Nov 01.2010 81:206–11. [PubMed: 20688491]
15. Ciofani G, Raffa V, Obata Y, Menciassi A, Dario P, Takeoka S. Magnetic driven alginate nanoparticles for targeted drug delivery. Current Nanoscience. May.2008 4:212–218.
16. Kondaveeti S, Cornejo DR, Petri DF. Alginate/magnetite hybrid beads for magnetically stimulated release of dopamine. Colloids Surf B Biointerfaces. Feb 01.2016 138:94–101. [PubMed: 26674837]
17. Massart R. Preparation of Aqueous Magnetic Liquids in Alkaline and Acidic Media. Ieee Transactions on Magnetics. 1981; 17:1247–1248.
18. Herrera AP, Barrera C, Rinaldi C. Synthesis and functionalization of magnetite nanoparticles with aminopropylsilane and carboxymethyldextran. Journal of Materials Chemistry. 2008; 18:3650–3654.
19. Jay SM, Shepherd BR, Bertram JP, Pober JS, Saltzman WM. Engineering of multifunctional gels integrating highly efficient growth factor delivery with endothelial cell transplantation. FASEB J. Aug.2008 22:2949–56. [PubMed: 18450813]
20. Jay SM, Saltzman WM. Controlled delivery of VEGF via modulation of alginate microparticle ionic crosslinking. J Control Release. Feb 20.2009 134:26–34. [PubMed: 19027807]
21. Mabille C, Schmitt V, Gorria P, Calderon FL, Faye V, Deminiere B, et al. Rheological and shearing conditions for the preparation of monodisperse emulsions. Langmuir. Jan 25.2000 16:422–429.
22. Schneider CA, Rasband WS, Eliceiri KW. NIH Image to ImageJ: 25 years of image analysis. Nat Methods. Jul.2012 9:671–5. [PubMed: 22930834]
23. Leng, DE., Calabrese, RV. Immiscible Liquid-Liquid Systems," in. In: Paul, EL.Atiemo-Obeng, VA., Kresta, SM., editors. Handbook of Industrial Mixing: Science and Practice. Hoboken, NJ USA: John Wiley & Sons; 2003.
24. Hall S, Cooke M, Pacek AW, Kowalski AJ, Rothman D. Scaling up of Silverson Rotor-Stator Mixers. Canadian Journal of Chemical Engineering. Oct.2011 89:1040–1050.
25. Masuelli MA, Illanes CO. Review of the characterization of sodium alginate by intrinsic viscosity measurements. Comparative analysis between conventional and single point methods. International Journal of Biomaterials Science and Engineering. 2014; 1:1–11.
26. Andereck CD, Liu SS, Swinney HL. Flow Regimes in a Circular Couette System with Independently Rotating Cylinders. Journal of Fluid Mechanics. Mar.1986 164:155–183.
27. Taylor GI. The formation of emulsions in definable fields of flow. Proceedings of the Royal Society of London Series a-Containing Papers of a Mathematical and Physical Character. Oct.1934 146:0501–0523.

28. Grace HP. Dispersion Phenomena in High-Viscosity Immiscible Fluid Systems and Application of Static Mixers as Dispersion Devices in Such Systems. Chemical Engineering Communications. 1982; 14:225–277.

29. Kiss N, Brenn G, Pucher H, Wieser J, Scheler S, Jennewein H, et al. Formation of O/W emulsions by static mixers for pharmaceutical applications. Chemical Engineering Science. Nov 1.2011 66:5084–5094.

30. Maa YF, Hsu C. Liquid-liquid emulsification by rotor/stator homogenization. Journal of Controlled Release. Feb.1996 38:219–228.

31. Rosensweig RE. Heating magnetic fluid with alternating magnetic field. Journal of Magnetism and Magnetic Materials. Nov.2002 252:370–374.

Highlights

- A methodology for preparing magnetic alginate microspheres with controllable sizes through an emulsification and ionic crosslinking process is proposed.
- Magnetic nanoparticles are incorporated in the alginate microspheres by mixing the nanoparticles with the alginate dispersed phase.
- Microsphere size can be manipulated by the homogenizer shear rate and the alginate volume fraction in the dispersed phase.
- Magnetic alginate microspheres respond to the application of a magnetic field and can form columnar structures under such.

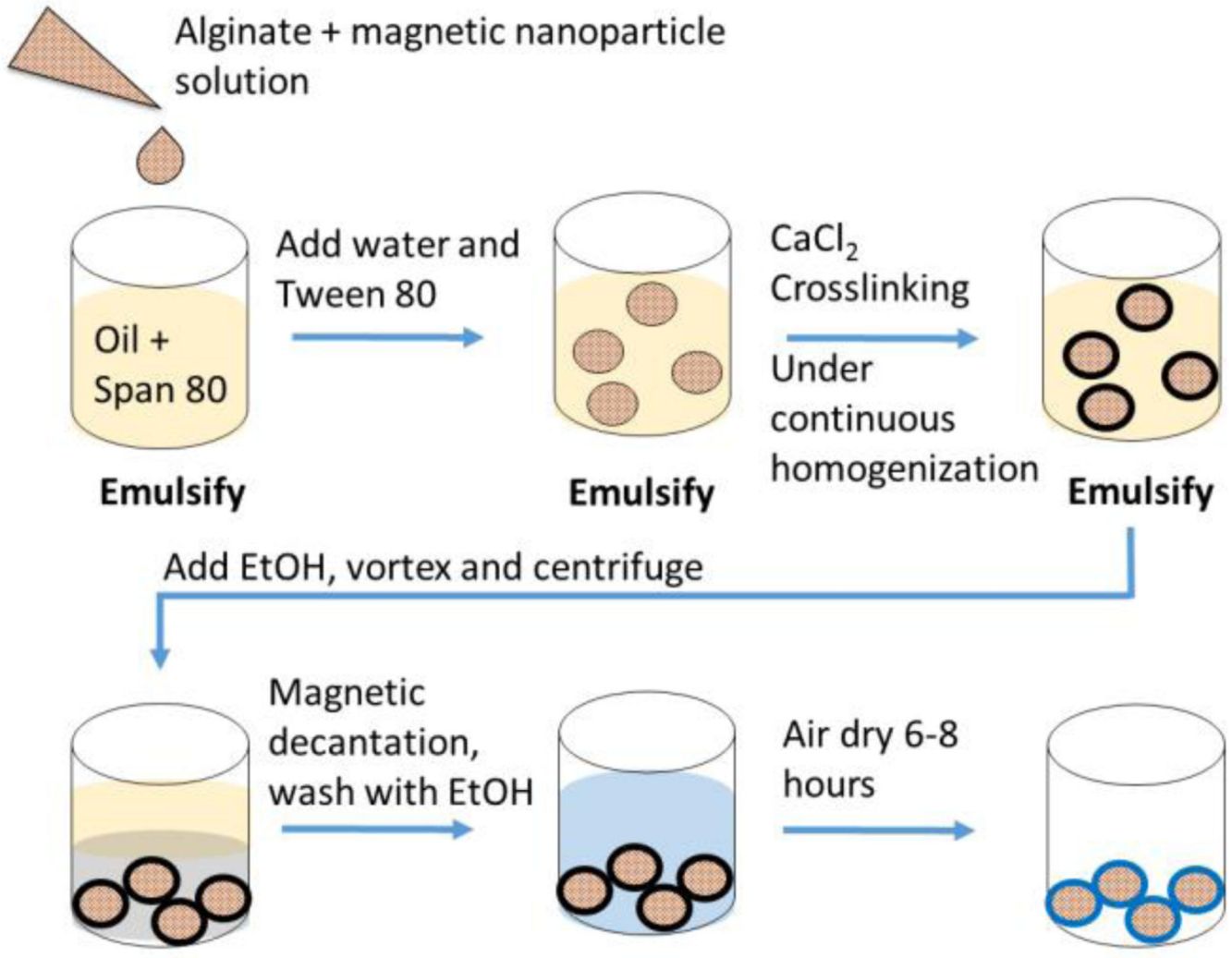

Figure 1.
Schematic of emulsification and ionic crosslinking process to make magnetic alginate microspheres.

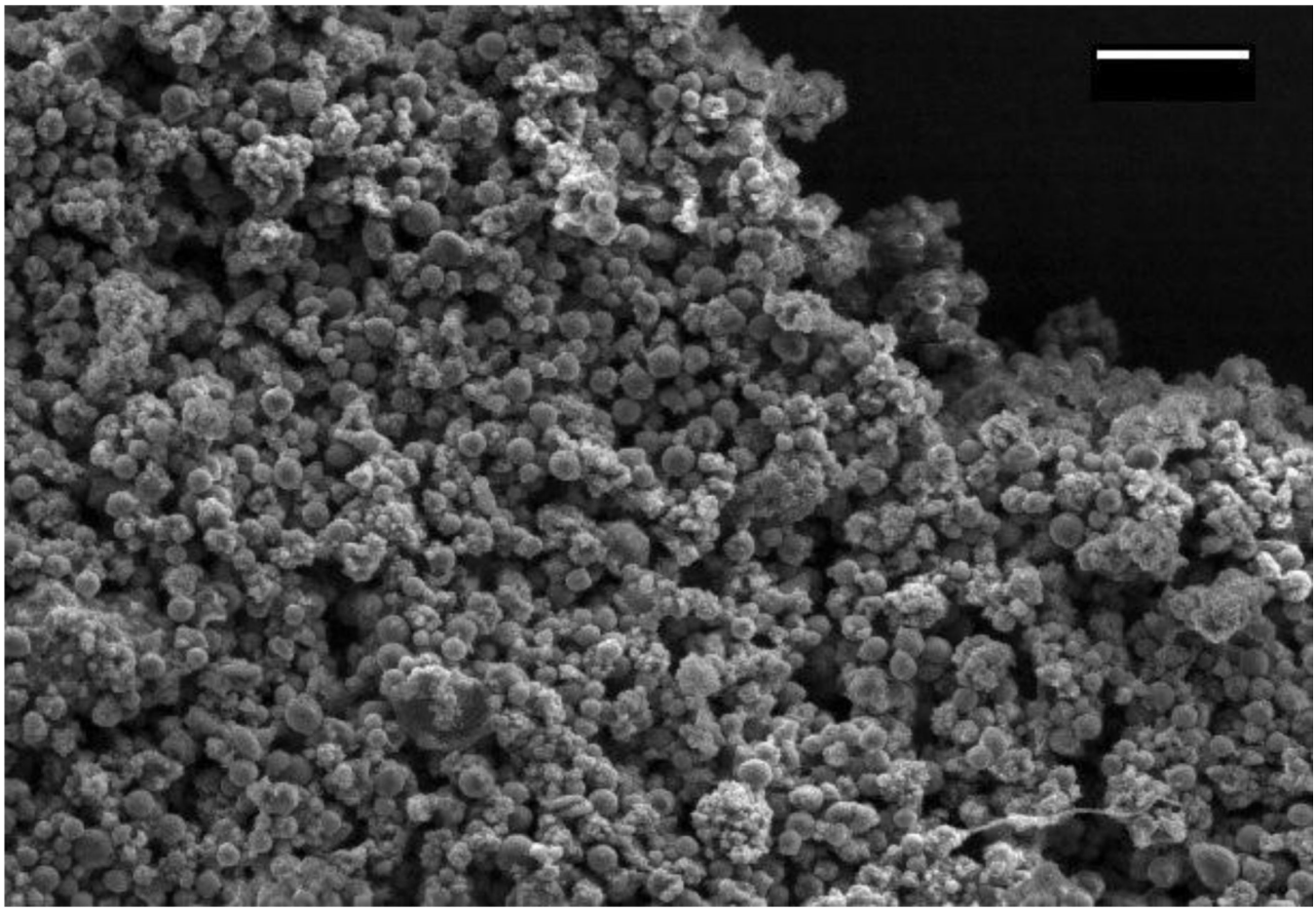

Figure 2.

Representative SEM image of magnetic alginate microspheres made by the emulsification and ionic crosslinking process described herein. These microspheres were made under an applied shear rate of 9400 s^{-1}, using an alginate volume fraction in the dispersed phase of 0.984% v/v, and 1 mL of a ferrofluid with a magnetic nanoparticle concentration of 16 mg/mL. Scale bar, 5 μm.

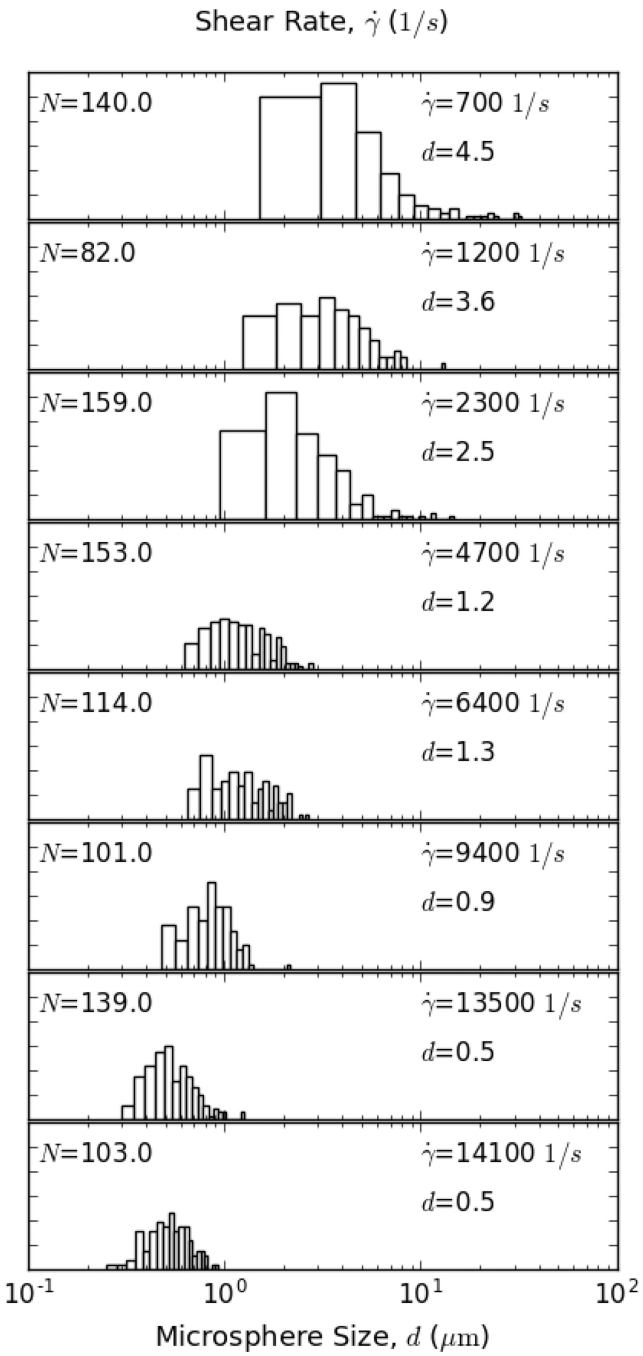

Figure 3.

Microsphere size histograms from microsphere preparations with varying shear rates made with alginate volume fractions of 0.984% v/v and using a high viscosity continuous phase. In this figure, N is defined as the sample size of analyzed microspheres, d is the median microsphere diameter in μm, and $\dot{\gamma}$ is the shear rate.

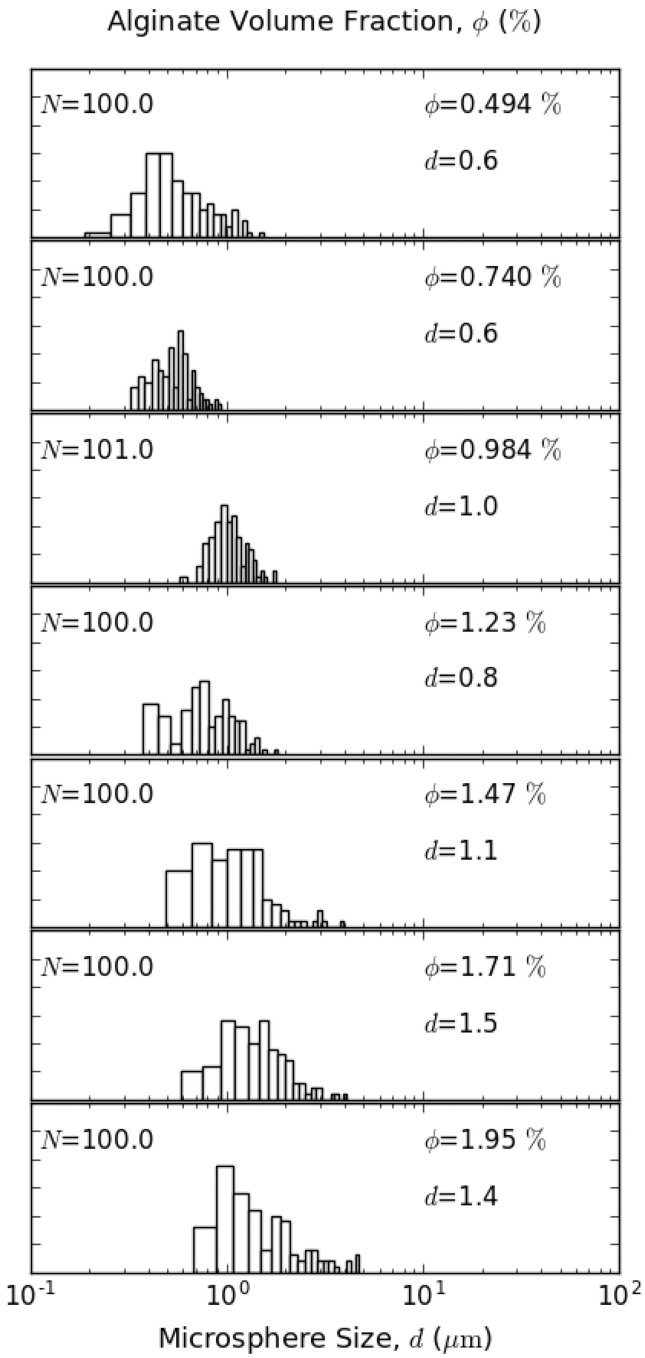

Figure 4.

Microsphere size histograms from microsphere preparations with varying alginate volume fractions made under applied shear rates of 9400 s^{-1} and using a high viscosity continuous phase. In this figure, *N* is defined as the sample size of analyzed microspheres, *d* is the median microsphere diameter in μm, and ϕ is the alginate volume fraction.

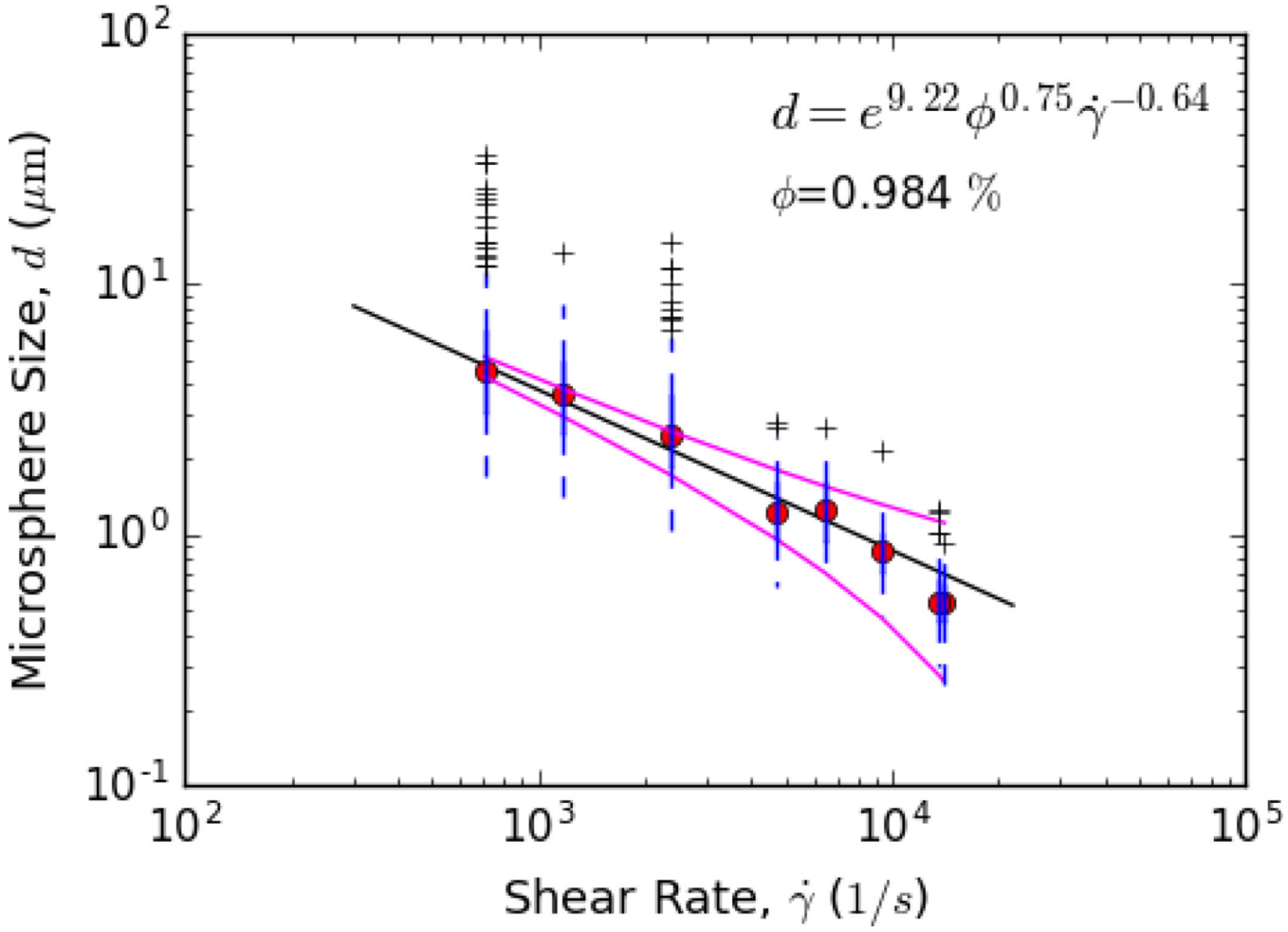

Figure 5.

Microsphere size reduction with increasing applied shear rates observed from magnetic alginate microsphere preparations made with alginate volume fractions of 0.984% v/v and using a high viscosity continuous phase. The curves above and below the regression line show the upper and lower 95% confidence limits of the fit, respectively.

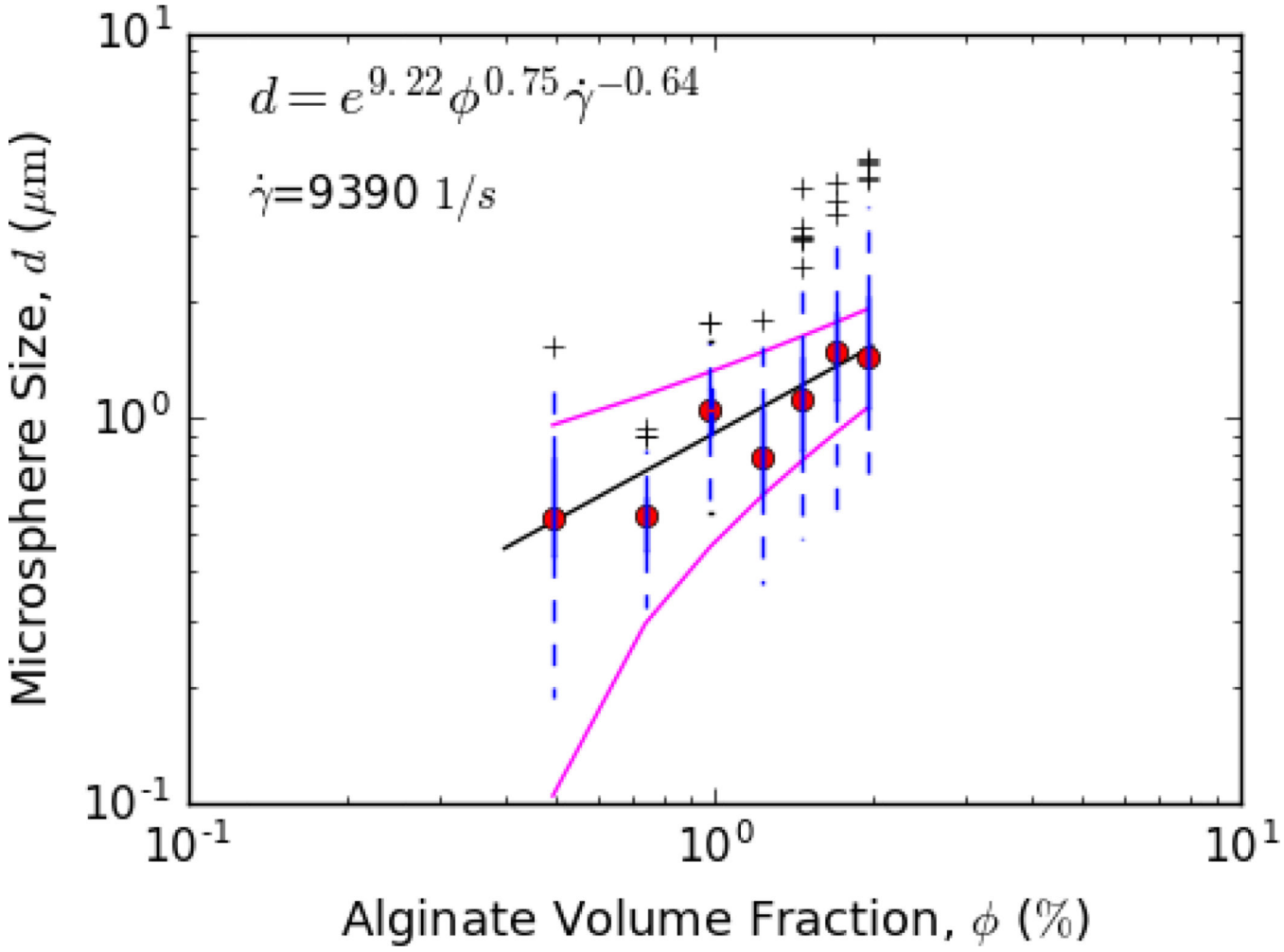

Figure 6.
Microsphere size increase with increasing alginate volume fractions on microsphere size observed from magnetic alginate microsphere preparations made under applied shear rates of 9400 s^{-1} and using a high viscosity continuous phase. The curves above and below the regression line show the upper and lower 95% confidence limits of the fit, respectively.

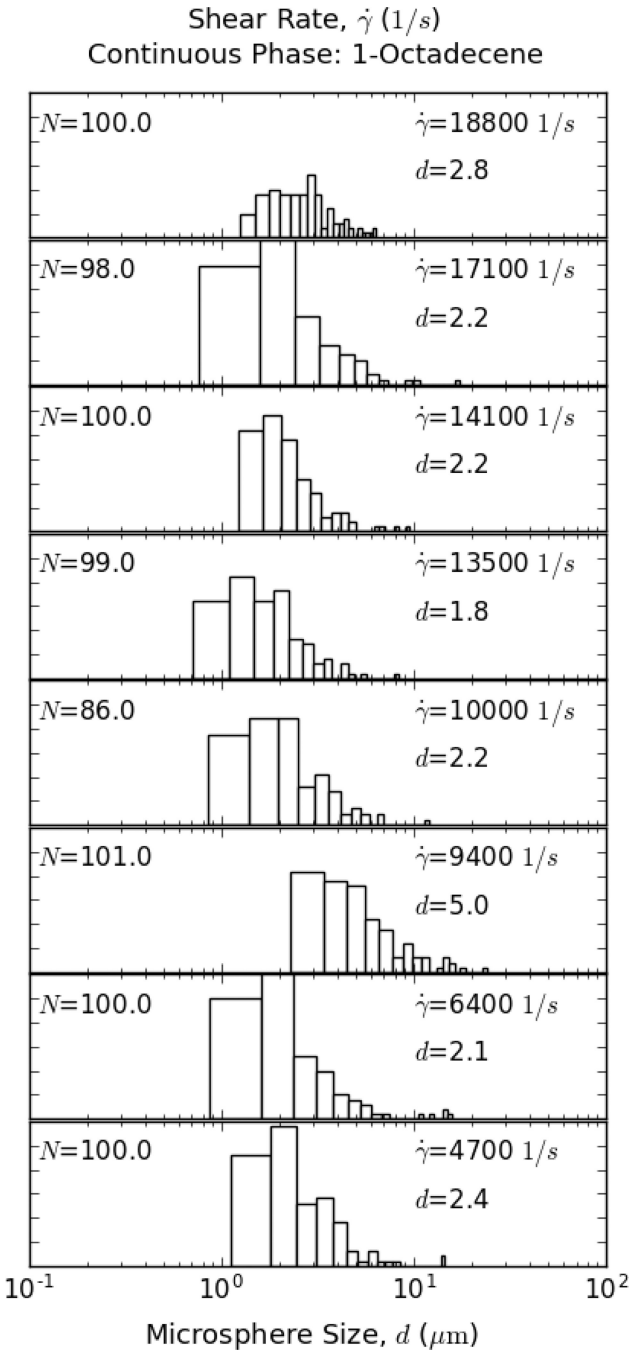

Figure 7.

Microsphere size histograms from microsphere preparations with varying shear rates made with alginate volume fractions of 0.984% v/v and using a low viscosity continuous phase. In this figure, N is defined as the sample size of analyzed microspheres, d is the median microsphere diameter in μm, and $\dot{\gamma}$ is the shear rate.

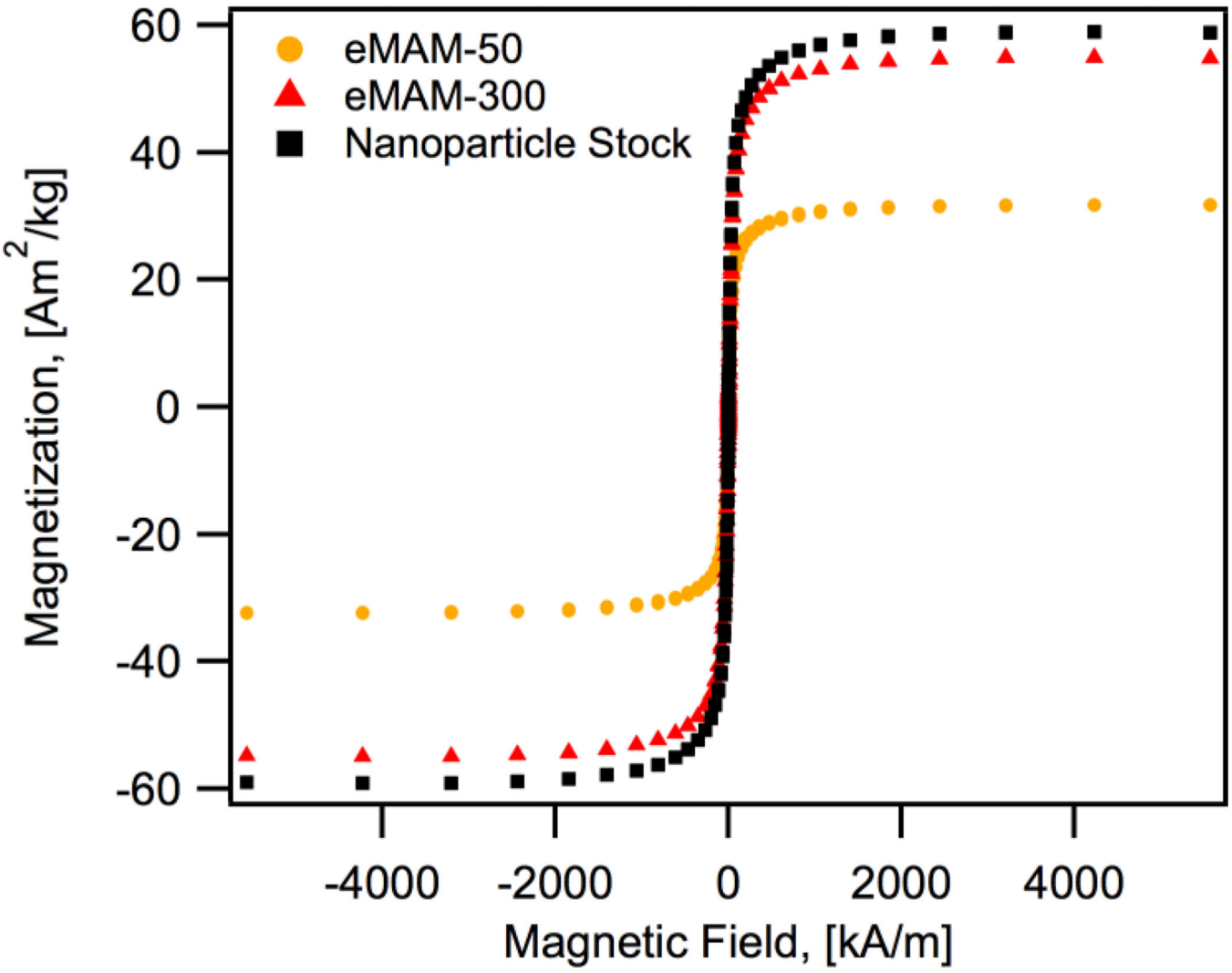

Figure 8.
Equilibrium magnetization curves at 300K for magnetic microspheres and the stock magnetic nanoparticles. The equilibrium magnetization curves of magnetic microspheres were normalized by the total mass of dry microspheres.

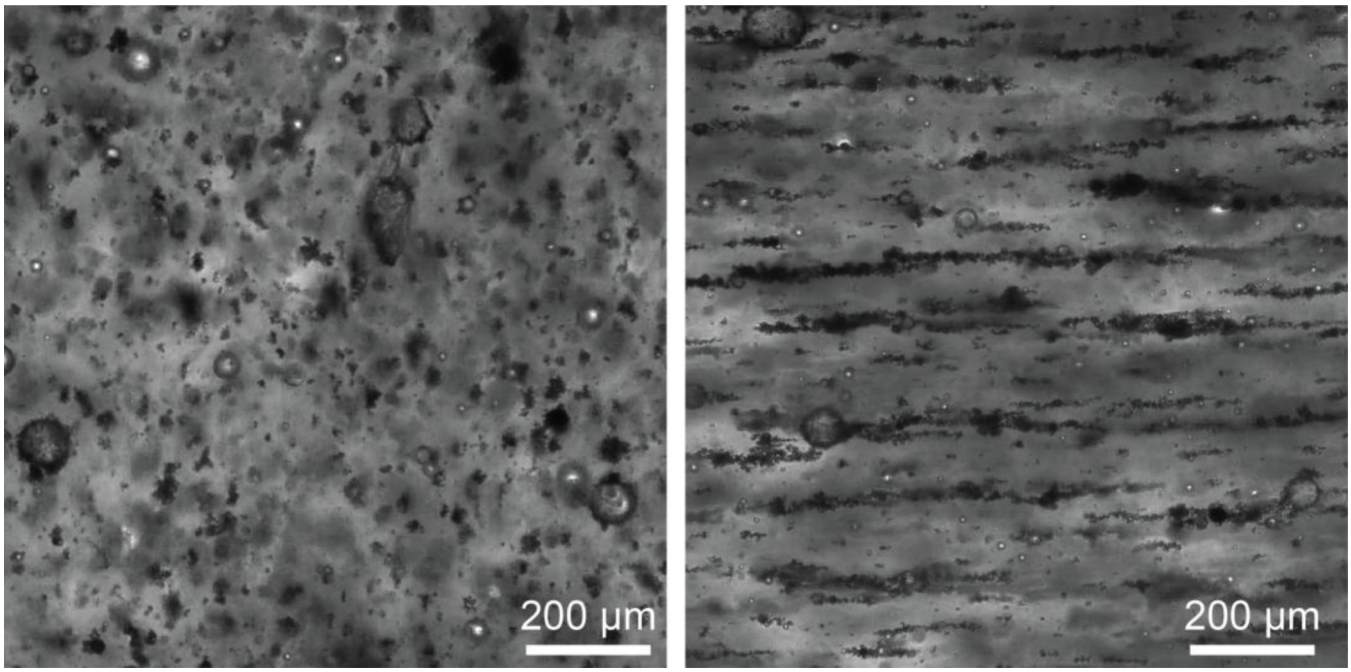

Figure 9.

Optical microscopy images of magnetic microspheres made with $\dot{\gamma} = 9400\ s^{-1}$ and $Z = 200$ mg/mL taken before (left) and after (right) the application of a magnetic field. Both images share the same scale bar of 200 μm.

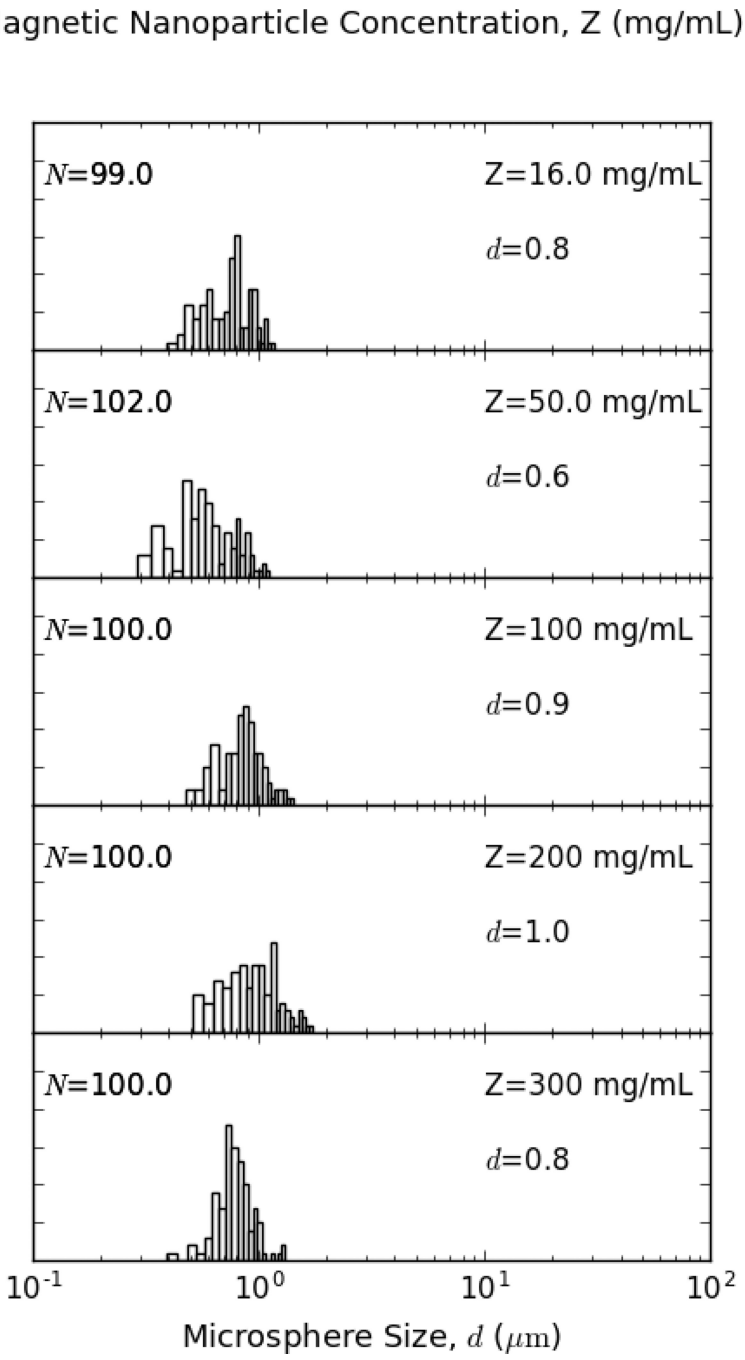

Figure 10.

Microsphere size histograms from microsphere preparations with different magnetic nanoparticle concentrations, made under applied shear rates of 9400 s^{-1}, with alginate volume fractions of 0.984% v/v and using a high viscosity continuous phase. In this figure, N is defined as the sample size of analyzed microspheres, d is the median microsphere diameter in μm, and Z is the magnetic nanoparticle concentration.

Table 1

Iron oxide mass fractions in magnetic alginate microspheres (MAMs) measured by the *o*-phenanthroline assay, estimated from the SQUID saturation magnetization, and estimated theoretically based on the mass of stock nanoparticles used in the preparation.

Sample	UV-Vis IO Mass Fraction (%) ± Std. Dev. (n = 3)	SQUID IO Mass Fraction (%)	Theoretical Mass Fraction
MAMs (50 mg/ml)	52 ± 3.5	54	56
MAMs (300 mg/ml)	85 ± 1.9	93	88

Note: 50 mg/ml and 300 mg/ml represent the concentrations of the stock ferrofluid